

The Stern Gerlach Experiment

Jeff Lieberman

Department of Physics, Massachusetts Institute of Technology

Cambridge, Massachusetts 02139

(June 22, 1998)

Abstract

In this paper we examine the Stern Gerlach experiment. We first take a theoretical look at the atom deflections in an inhomogeneous magnetic field, and we compare classical and quantum expectations for these deflections, using the Maxwell-Boltzmann distribution of atom velocities. We then describe the experimental setup the analysis of our results. We use the Stern Gerlach experiment to definitively show the existence of the quantization of angular momentum. The splitting of the beam confirms our expectations, to an extreme level of confidence. We use the same molecular beam techniques to determine the magnetic moment of Potassium, which we find to be $(9.0 \pm 0.6) \times 10^{-24}$ J/T, well within the expected error of the accepted value of 9.285×10^{-24} J/T.

I. INTRODUCTION

We have known since the discovery of the Zeeman effect that atoms have magnetic dipole moments. Bohr's theory supposed the quantization of angular momentum, and therefore the magnetic moment, but assumed only circular orbits. Sommerfeld later furthered this theory to include elliptical orbits, and initiated the use of the description of these states by the three quantum numbers, n, k , and m . n referred to the normal Bohr quantum number, and k determined the geometry of the orbits. m determined the projection of the angular momentum vector along any axis, which took on only a discrete set of values. Sommerfeld's theory could account for both the fine structure of hydrogen, as well as the normal Zeeman effect. However, there was still question to as whether there truly did exist such a spatial quantization.

Otto Stern, in 1921, thought of a conclusive experiment to find the answer to this question. He proposed to observe the deflection of a beam of neutral silver atoms in an inhomogeneous magnetic field. The deflection would be caused solely by the nuclear magnetic moments. He assumed that, since silver has one valence electron, $m = \pm 1$ in the ground state. If there were a random orientation of the magnetic moments, then the distribution of the deflections would decrease monotonically from the center outward. If space quantization existed, the beam should be split into two distinct beams, corresponding to parallel and anti-parallel alignments of the magnetic moments. Stern enlisted the help of Walter Gerlach to coordinate the experiment. After one year of experimentation, they finally observed the result: a beam splitting of approximately 0.2 millimeters.

In 1926, the more advanced theories of quantum mechanics showed a mistake in Stern's analysis: The ground state of the silver atom actually had zero orbital angular momentum. The moment that had been observed was that of the intrinsic spin angular momentum, the first quantum variable with no classical analog. It is interesting to note that had Stern chosen an atom of orbital angular momentum nonzero, the beam would have been split further, and the effect would have been unobservable. Otto Stern later, in 1943, won the

Nobel prize in physics for this and related work.

II. THEORY OF THE STERN GERLACH EXPERIMENT

An electron in a circular orbit has a classical angular momentum $\mathbf{L} = m\omega r^2$, and a magnetic moment given by $\mu = -(e/2m_e)\mathbf{L}$, where m and e are the mass and charge of the electron, and r and ω are the radius and angular velocity of the motion. If this atom is placed inside a magnetic field, strongly varying in magnitude along the z -axis, the atom will experience a force $F_z = -\nabla(-\mu \cdot \mathbf{B}) = \mu_z \partial B_z / \partial z$, which can range continuously over all values such that $|F_z| \leq |\mu| \partial B_z / \partial z$. If classical mechanics was applicable in this situation, then we should see a distribution of deflection angles, with a maximum at zero deflection, and decreasing outward in each direction. But, this is not what is seen.

In quantum mechanics, an atom in this situation can exist in an eigenstate of the Hamiltonian only if it has a definite value of $\mathbf{F} \cdot \mathbf{F}$, its total angular momentum, and a definite value of the component of the angular momentum about any axis (here we choose the z axis, \mathbf{F}_z). These two quantities are only allowed certain values,

$$\mathbf{F} \cdot \mathbf{F} = f(f+1)\hbar^2 \text{ where } f \text{ is an integer or half integer,} \quad (1)$$

and

$$\mathbf{F}_z = m_z \hbar, \quad (2)$$

where m_z can take only the values $-f, -f+1, \dots, f-1$, or f . We associate with this angular momentum a magnetic moment given by $\mu = -g_f(e/2m_e c)\mathbf{F}$, where g_f is the Landé g-factor. Thus, the projection of the angular momentum onto the z -axis can take only the discrete set of values $\mu_z = g_f m_z \mu_B$, where μ_B is the Bohr magneton, given by $\mu_B = e\hbar/2m_e c$. Now, if once again the atoms are placed into the same magnetic field, the force will have only a set of discrete values which are allowed, $F_z = m_z g_f \mu_B (\partial B_z / \partial z)$. Thus, a beam of particles with a value of $\mathbf{F} = \sqrt{f(f+1)}\hbar$ of the angular momentum will be split into $2f+1$ beams, corresponding to each possible value of m_z .

We proceed to analyze our present situation, the Stern Gerlach experiment. In our experiment, a beam of potassium atoms is passed through an inhomogeneous magnetic field. Our total angular momentum is the sum of the spin and the orbital angular momenta, the latter referring to the motion of the electrons around the nucleus. We designate the ground state of Potassium as $^2S_{1/2}$, meaning that the atom is in the S-state (where $\mathbf{L} = 0$), the fine-structure degeneracy of higher states is two (the unpaired electron can have either spin up or down), and the total electron angular momentum $\mathbf{J} = \mathbf{L} + \mathbf{S} = (1/2)\hbar$, where \mathbf{S} represents the spin angular momentum. The magnetic moment associated with the electron spin is $-g_s\mu_B\mathbf{S}/\hbar$, where $g_s = 2.0023$ is the gyromagnetic ratio of the electron. The nuclear angular momentum of ^{39}K (the most abundant isotope) is $\mathbf{I} = (3/2)\hbar$, and the nuclear magnetic moment is $g_n\mu_B\mathbf{I}/\hbar$, where $g_n \ll g_s$. In space, the interaction between the magnetic moments \mathbf{J} and \mathbf{I} causes a rapid precession about the total angular momentum axis, \mathbf{F} . The quantum number of the sum is $f = i \pm j = 1$ or 2 . For each possibility, we associate a different magnetic moment.

In our setup, at temperatures of 200°C , almost all of the potassium atoms will be in the ground state of energy, and will be equidistributed among the two possible angular momentum states, $f = 1$ and 2 . Within these two states there will be a near equal distribution of the hyperfine states (different m_z). If we apply a beam of these atoms to a weak magnetic field, we will see a splitting of the beam into as many beams as there are different values of m_z . We use a strong magnetic field, in which \mathbf{I} and \mathbf{J} are decoupled, and both precess independently about the direction of \mathbf{B}^1 . The magnetic moment is now approximately $\mathbf{J}=\mathbf{S}$ ($\mathbf{L}=0$), which can have only two projections in the direction of the field, $\mu_z = \pm g_s\mu_B/2$. The beam is thus split into two main beams, split by the possible values of \mathbf{S} , each having a hyperfine splitting caused by \mathbf{I} that we are unable to resolve with our experimental

¹We have not explained the reason for the decoupling. For an explanation of this and a more rigorous treatment of the quantum mechanics involved, see Appendix 1.

equipment.

A. Atom Deflection by a Non-Uniform Magnetic Field

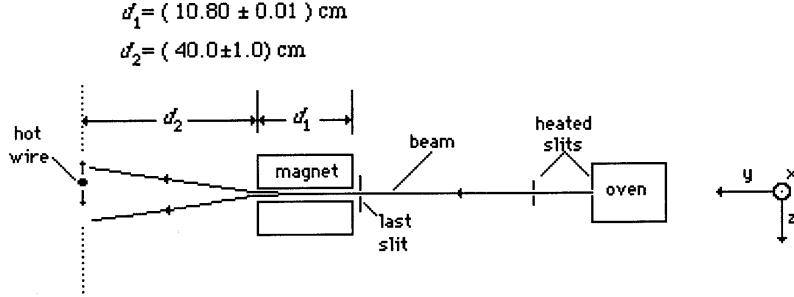


Figure 1: Top view of the experimental apparatus used in the Stern Gerlach experiment

The apparatus for the experiment is shown in Figure 1. The beam is directed along the y -axis, and splits slightly along the z -axis. We can calculate the deflection of an atom with mass m and velocity v by assuming that the deflecting force is constant in the region of the beam, and zero everywhere else. If we call the deflection z , then from Newton's law we have

$$z = \frac{1}{2}a_z t_1^2 + v_z t_2 = \frac{1}{2} \frac{F_z}{M} \left(\frac{d_1}{v_y} \right)^2 + \frac{F_z}{M} \left(\frac{d_1}{v_y} \right) \left(\frac{d_2}{v_y} \right) \quad (3)$$

where $t_1(= d_1/v_y)$ and $t_2(= d_2/v_y)$ denote the time spent in the magnetic field, and the time spent after the field, before hitting the detector, respectively. Using the approximation that $v_y \approx |v|$, because the motion is almost exclusively in the y direction, we obtain our expression for z ,

$$z = \frac{F_z}{mv^2} d_1 \left[\frac{d_1}{2} + d_2 \right]. \quad (4)$$

B. Atom Velocity Distributions

As is obvious from experiment, we do not achieve a delta-function type peak at each of the expected deflection points. Rather, there is a bimodal distribution. The primary cause of

this is the distribution of particle velocities when leaving the oven, which follow a Maxwell-Boltzmann distribution. According to Maxwell-Boltzmann statistics, the fraction of atoms with velocities between V and $V + dV$ in the oven is

$$f(V)dV = \frac{4}{\sqrt{\pi}} \left(\frac{V}{V_0}\right)^2 e^{-\left(\frac{V}{V_0}\right)^2} d\left(\frac{V}{V_0}\right), \quad (5)$$

where $V_0 = \sqrt{2kT/m}$ is the most probable velocity of the atom ($kT = (1/2)mV_0^2$). The flux of atoms that emerge through the slit with velocities between V and $V + dV$ is proportional to the product of the number density of such atoms with the velocity with which they leave the oven. Normalizing the flux $I(V/V_0)$, we therefore have

$$I\left(\frac{V}{V_0}\right) d\left(\frac{V}{V_0}\right) = 2\left(\frac{V}{V_0}\right)^3 e^{-\left(\frac{V}{V_0}\right)^2} d\left(\frac{V}{V_0}\right). \quad (6)$$

This distribution of velocities gives rise to the distribution in deflection, which we will now calculate.

C. Deflection Distributions for a Quantized Deflection Force

Let us denote by $I(z)dz$ the fraction of atoms that are deflected between a range of z and $z + dz$. By taking the logarithmic derivative of equation ??, we obtain

$$\frac{dz}{z} = -2\frac{dV}{V}. \quad (7)$$

Setting

$$I(z)dz = -I\left(\frac{V}{V_0}\right) d\left(\frac{V}{V_0}\right),$$

and following through with algebra, we can combine the above to obtain

$$I(z)dz = I_0 \left(\frac{z_0}{|z|}\right)^3 e^{-z_0/|z|} d(z/z_0), \quad (8)$$

where z_0 is defined as the deflection of an atom with the average velocity V_0 . The maxima of this function occur at $\pm z_0/3$.

In our experiment, the z -component of the force is restricted to two discrete values, as described above, and this then leads to two possible values for the deflection, namely (from eq. (??))

$$z_0 = \pm(1/2)g_s\mu_B \frac{\partial B_z}{\partial z} \left[d_1(d_2 + d_1/2)/MV_0^2 \right] \quad (9)$$

So, we expect the beam to split into two components, with the beam heading towards points $\pm z$, nearly equally distributed in intensity. We will not be focusing on the magnitudes of the intensities, just on the overall shape, which will yield be sufficient to yield us values for the source temperature, as well as the multiplicity of magnetic substates and the magnitude of the magnetic moment of the potassium atom.

D. Deflection Distribution for Randomly Oriented Magnetic Moments

To be sure that our measurments are truly evidence of quantum effects, we would like to compare the theory presented above to a classical analysis of the same problem. Consider a beam of atoms with dipole moments distributed uniformly in direction, each with the same magnitude. Each atom will have a projection of the moment onto the z -axis of value $\mu_B \cos\theta$, as shown in Figure 2.

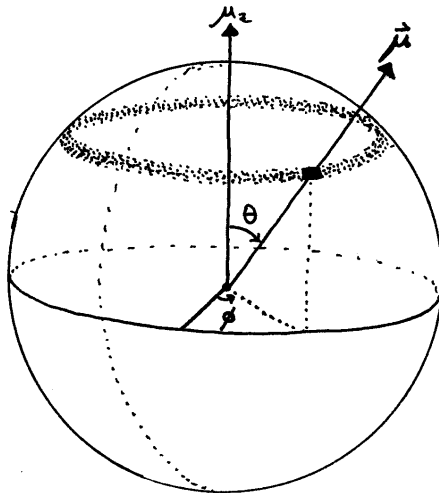


Figure 2: Randomly oriented (classical) magnetic moments

The fraction of atoms within θ and $\theta + d\theta$ is $1/2\sin\theta d\theta = -1/2d\cos\theta$, and this fraction will be deflected with the distribution given in equation (??) , where we now have z_0 replaced by $z_0\cos\theta$. Therefore, the fraction of atoms deflected by the amount z to $z + dz$ is given by

$$\begin{aligned} I(z)dz &= -\frac{dz}{2z_0} \int_0^{\pi/2} \left(\frac{z_0\cos\theta}{z} \right)^2 e^{-\left(\frac{z_0\cos\theta}{z}\right)} d\left(\frac{z_0\cos\theta}{z} \right) \\ &= \frac{dz}{2z_0} \int_0^{z_0/z} u^2 e^{-u} du \\ &\propto \left(1 - \left[1 + \left(\frac{z_0}{|z|} \right) + \frac{1}{2} \left(\frac{z_0}{|z|} \right)^2 \right] e^{-\frac{z_0}{|z|}} \right) dz. \end{aligned} \quad (10)$$

Figure 3 illustrates the difference between the classical and quantum expectations. This reinforces the fact that what we observe is definitely a quantum effect, something which classical mechanics cannot describe.

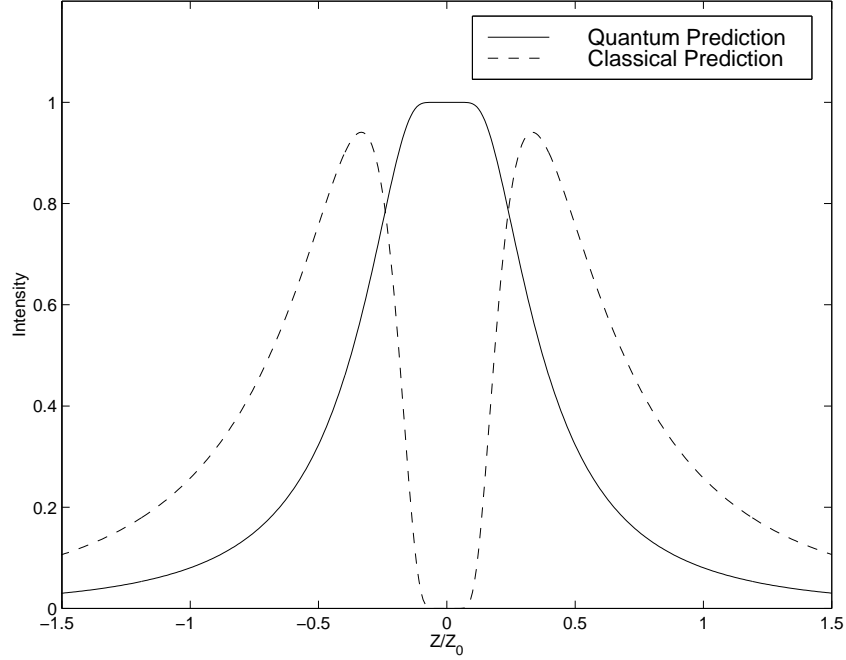


Figure 3: Comparison of classical and quantum mechanical predictions of beam spreading, where our beam has $j = 1/2$

E. Beam Width Contribution to the Deflection Distribution

In our above analysis we have neglected the fact that the beam of Potassium atoms has a finite width, and also has an angular divergence. The current measured at a position z

has contributions from atoms that have suffered deflections comparable to the width of the beam, because the deflection is only slightly greater than the width of the undeflected beam. We call $g(u-z)dz$ the fraction of atoms that have been deflected by an amount u that arrive between z and $z + dz$. Then we have the fraction of atoms arriving between z and $z + dz$ expressed by a convolution integral:

$$I(z) = \int_{u=-\infty}^{+\infty} I(u)g(z-u)du \quad (11)$$

This ignores higher order effects of atomic collisions within the beam. These effects are small and are not considered in the analysis. We also assume that $g(\gamma)$ is independent of z . If we use our zero-field calculation to determine $g(\gamma)$, we can then convolve that beam spread function with our other data in order to find the intensity function I and therefore find values of z_0 .

Eq. (??) gives us, solving for the magnetic moment (using the fact that $1/2mV_0^2 = 3/2kT$, where $k = 1.38 \times 10^{-23} J/K$ is the Boltzmann constant)

$$\mu_K = \frac{3z_0kT}{\frac{\partial B_z}{\partial z} [d_1d_2 + d_1^2/2]}. \quad (12)$$

With this is an associated error of

$$\Delta\mu_K = \mu_K \sqrt{\left(\frac{\Delta z_0}{z_0}\right)^2 + \left(\frac{\Delta T}{T}\right)^2 + \left(\frac{\Delta \frac{\partial B_z}{\partial z}}{\frac{\partial B_z}{\partial z}}\right)^2 + \left(\frac{d_2 + d_1}{d_1d_2 + d_1^2/2} \Delta d_1\right)^2 + \left(\frac{d_1}{d_1d_2 + d_1^2/2} \Delta d_2\right)^2} \quad (13)$$

$$\approx \mu_K \left| \frac{\Delta \frac{\partial B_z}{\partial z}}{\frac{\partial B_z}{\partial z}} \right|, \quad (14)$$

because the error in our magnetic field calculation is much greater than our error in any other of our measurements.

III. SETUP AND PROCEDURE

The Potassium ^{39}K atoms begin inside an oven, in a solid slug which is gradually vaporized by heat. The atoms bounce inside the oven until they head in the direction of the oven opening. Upon leaving the opening, a tiny fraction of the departing atoms are directed in

the direction of two aligned slits. Those that pass through these two slits form a narrow beam that heads through the magnetic field. In order to create a dense beam, we need the mean free path of the atoms in the oven to exceed the width of the slit. To do this, we keep the oven in the temperature range of about $190 \pm 5^\circ K$. We monitor the temperature with a digital thermometer. The flux of atoms passing through the slit is highly dependent on the temperature of the oven, so it was necessary to wait approximately 90 minutes in order to insure temperature stability.

When the atoms have passed through the two slits, they head towards the electromagnet. In the entire region of the atoms travel, we keep them in a high vacuum in order to eliminate most of the collisions between the Potassium atoms and the surrounding air. The vacuum pressure ² is regulated by a turbomolecular pump, and is kept at approximately $< 10^{-6} torr$. The atoms, traveling through this near-vacuum, then enter the electromagnet region.

The electromagnet is made up of two iron pole pieces, wound in series on a C-yoke. They are oriented in order to create a very non-uniform magnetic field, with an approximately constant field gradient in the gap between the two pole pieces. We calculate the field gradient in terms of the observed magnetic field, which we can find from a measurement of the magnet current ³, which is measured on a Weston ammeter connected in series with the two coils.

In order to insure that we can accurately find the magnetic field from a measurement of the current, we must be sure to place the magnets on a known hysteresis curve. We do so by degaussing the magnet: by varying the current between $\pm 5amps$, and then leaving it at

²The exact value of the pressure is unimportant to us in this analysis. The lower pressure only helps us to gain more atomic hits, and therefore implicitly leads to a contribution in our overall error.

³A further description of the geometry, as well as a derivation for the gradient calculation, can both be found in Appendix 2.

a current of 0.65amps , we can be sure of leaving the field at less than 20gauss , negligible in comparison to our other errors. To set other values of the field, we first vary our current between $\pm 5\text{amps}$, and then we increase it monotonically to the desired level. This insures we remain on the hysteresis curve that we use for our data.

The atoms are detected by a 4 mil diameter platinum wire, kept at a temperature of about 1300°C , which is constantly biased at a voltage of approximately 15 volts. If the Potassium atoms hit the wire, they are quickly ionized (the work function of platinum is greater than the ionization energy of ^{39}K). We operate the wire at a current of 0.53 ± 0.01 A. The wire is first cleaned before each run by applying a 0.7 A current. The bias voltage quickly pulls the ions to a nearby rectangular plate, and this current is led through a shielded coaxial cable, where it is detected by an electrometer. (more detail necessary?) The wire can be swept through a maximum range of ≈ 6 cm, although the usual effected range is < 1 cm. We sweep slowly to insure that the detector does not produce hysteresis effects (i.e. a run backwards should give us the same beam profile).

We measure the beam profile for several values of the applied current, and from this deduce the magnetic moment of Potassium. First we find the optimum settings for the oven temperature and the wire current. The value of the temperature does not greatly affect measurement, so as long as it remains constant throughout a run, we encounter no difficulties. We keep the oven at $463 \pm 0.5^\circ\text{C}$. The value of the wire current is more important. Too high a current causes a high background electrometer reading, and too low a current causes a drastically slower detector response. We choose a current of .54 A for our measurements.

We then find the optimal beam position. For accurate measurements, we must know exactly where inside the magnet gap the atomic beam is traveling. To accomplish this, we first laterally slide the beam back and forth along the z axis. The measurement of the beam will respond based on what fraction of it is traversing the gap, and what part is getting blocked. We stop when we measure a maximum electrometer reading. We then rotate the oven until once again we find a maximum value. By varying these two displacements, we

can find (in time) an overall maximum reading. We then can laterally move the oven and find the boundaries of the magnet gap. We then take our position to be the average of the two gap boundaries.

We take the first run of data without any applied field. This gives us the natural beam profile, which is used as $g(\gamma)$ in eq. (??) for the convolution of later data. Data is captured from the electrometer reading into both a plotter and a PC. The plotter is used only for the initial tesing and optimization, and the data from the computer is analyzed to determine values for the deflection based on different applied currents. We then take beam profile readings for different values of the applied current.

IV. RESULTS AND ANALYSIS

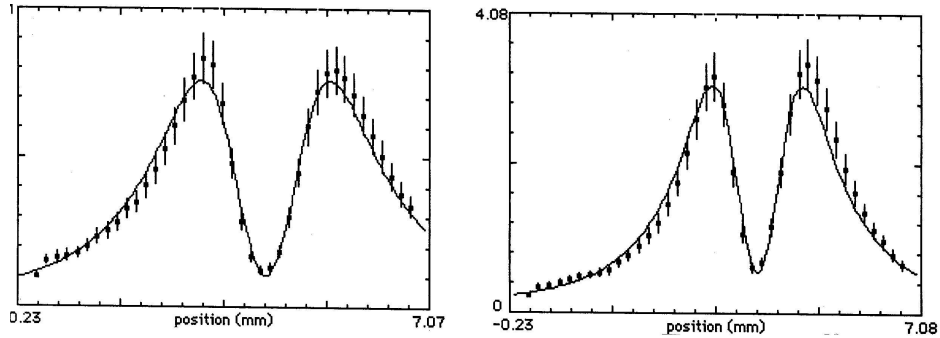


Figure 4: Samples of data collected with the Macintosh program *Stern.Gerlach.lsq Apl*, written by George Clark.

Figure 4 shows two samples of our data. We found the beam profiles for 5 different applied currents (listed with gradient calculations in Appendix B), in the range of 1 to 5 A. We meaasure the field gradient $\frac{\partial B_z}{\partial z}$ to be in the range from 61 to 120 T/m. As can be seen in Figure 5, As we increase the applied current, and hence the field gradient, the beam begins to split into two separate beams.

Trial #	Temperature(K)	$\frac{\partial B_z}{\partial z} (T/m)$	$z_0(cm)$	$\mu_k(J/T) \times 10^{-24}$	Estimated error
1	$463 \pm .5$	61.3 ± 8.0	0.134	8.48	13.1%
2	$463 \pm .5$	92.6 ± 11.7	0.205	8.58	12.6%
3	$463 \pm .5$	109.0 ± 13.6	0.257	9.15	12.5%
4	$463 \pm .5$	121.3 ± 15.1	0.294	9.40	12.4%

TABLE I. Summary of data obtained in the Stern Gerlach Experiment

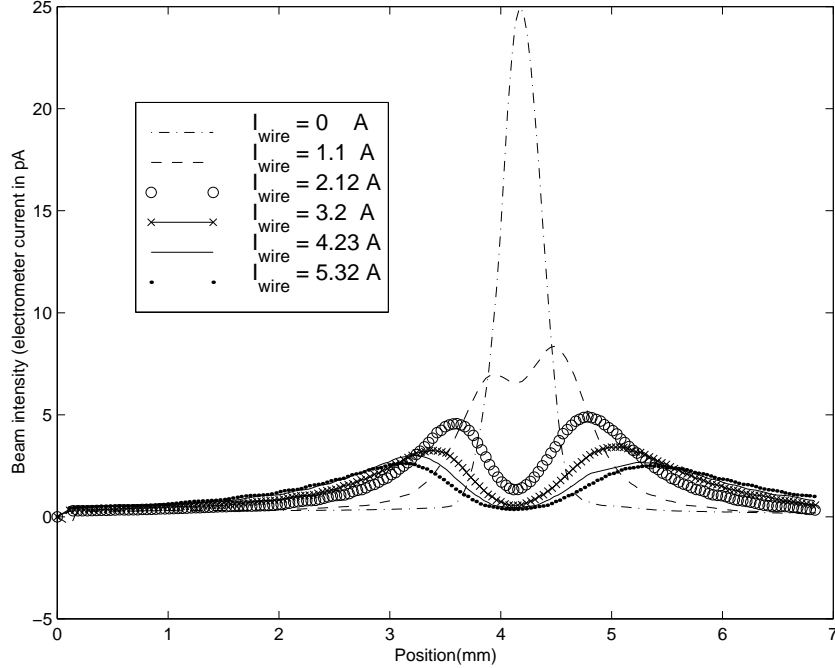


Figure 5: Resulting beam profiles for different current values.

The overall results of our calculations for different runs are shown in Table 1. Our error is primarily from the uncertainty in our position in the magnet gap, which we determined to an accuracy of about $w/6 \approx 0.05cm$, a conservative estimate. We have ignored the beam profile for the 1.1 A current, as it was greatly asymmetric, and we did not (due to calibrations) have time to retake this measurement. This run was asymmetric due to a high setting of drift speed of the detector.

We then proceed to statistically combine our data to find a final value for the magnetic

moment of Potassium. Using the formulas

$$\langle \mu_K \rangle = \frac{1}{n} \sum_n (\mu_K)_n \text{ and } \Delta \mu_K = \mu_K \frac{1}{\sqrt{\sum_i \frac{\mu_i^2}{\Delta \mu_i^2}}}, \quad (15)$$

we find $\mu_K = (9.0 \pm 0.6) \times 10^{-24}$ J/T, within the expected error of the accepted value of 9.285×10^{-24} J/T.

V. ACKNOWLEDGMENTS

I send an acknowledgement to George Clark for the data analysis program, and one great acknowledgement to Jeff Lieberman, in his unerring efforts to set over three different errors in this lab guide to rest. Thanks, me!

REFERENCES

- [1] Bohm, D., *Quantum Theory* (Prentice Hall, NJ, 1951)
- [2] Jackson, J.D. *Classical Electrodynamics* (Wiley, NY, 1962)
- [3] Ramsey, N.F. *Molecular Beams* (Oxford University, London, 1956)
- [4] Junior Lab Guide: *The Stern Gerlach Experiment*
- [5] I also looked up the original Stern Gerlach Paper, but it was in German, so not too useful for me.

APPENDIX A: A MODERN ANALYSIS OF THE STERN GERLACH EXPERIMENT

A more rigorous and modern quantum treatment of the Stern Gerlach experiment is valuable for several reasons. First, it gives a familiar example in which quantum measurement plays a key role. Only a modern view of the experiment gives deep links between the dynamics of the system and the mechanism of quantum measurement. Second, the Hamiltonian is easy to solve, and moreover the rigorous mathematical solution will give us an insight into the magnetic moment decoupling that we take for granted in our analysis, but which is key to our peak observations. It also reveals how the beam splitting manifests itself macroscopically.

We begin with the beam of particles (spin 1/2), passing through our non-uniform magnetic field, traveling on what we define as the x axis. The Schrödinger equation for this system is

$$\mathcal{H}|\Psi\rangle = i\hbar \frac{\partial}{\partial t} |\Psi\rangle, \quad (1)$$

where the Hamiltonian is given by

$$\mathcal{H} = \frac{p^2}{2m} + \frac{g\mu_B}{\hbar} \mathbf{S} \cdot \mathbf{B}(\mathbf{x}), \quad (2)$$

where \mathbf{S} is the spin operator, $\mathbf{B}(\mathbf{x})$ is the magnetic field at point \mathbf{x} , μ_B is the Bohr magneton, and g is the gyromagnetic ratio.

We consider the idealization (more than enough accuracy for our calculations) that the magnetic field is perpendicular to the motion of the electrons, i.e. $B_x = 0$. The direction of the field measured on the axis is taken to be the z axis, so $B_y = 0$. We find the field that satisfies these two properties as well as Maxwell's equations $\nabla \cdot \mathbf{B} = 0$ and $\nabla \times \mathbf{B} = 0$. We find a solution to be

$$\mathbf{B}(\mathbf{x}) = \beta y \hat{\mathbf{j}} + (B_0 - \beta z) \hat{\mathbf{k}}. \quad (3)$$

We have our wavefunction that satisfies the projection

$$\langle \mathbf{x} | \Psi \rangle = \begin{pmatrix} \Psi_+(\mathbf{x}, t) \\ \Psi_-(\mathbf{x}, t) \end{pmatrix}. \quad (4)$$

The spin operator in this system is

$$\mathbf{S} = \frac{\hbar}{2} \begin{pmatrix} 0 & 1 \\ 1 & 0 \end{pmatrix} \hat{\mathbf{i}} + \frac{\hbar}{2i} \begin{pmatrix} 0 & 1 \\ -1 & 0 \end{pmatrix} \hat{\mathbf{j}} + \frac{\hbar}{2} \begin{pmatrix} 1 & 0 \\ 0 & -1 \end{pmatrix} \hat{\mathbf{k}}. \quad (5)$$

If we substitute these facts into eq. (??), we get two Schrödinger equations,

$$-\frac{\hbar^2}{2m} \nabla^2 \Psi_{\pm} \pm \frac{g\mu_B \beta y}{2i} \Psi_{\mp} \pm \frac{g\mu_B}{2} (B_0 - \beta z) \Psi_{\pm} = i\hbar \frac{\partial \Psi_{\pm}}{\partial t}. \quad (6)$$

Now we need to show that the spinor components decouple. From the Heisenberg picture, we have

$$\frac{d\mathbf{S}}{dt} = \frac{1}{i\hbar} [\mathcal{H}, \mathbf{S}] = \frac{-\mu_B g}{\hbar} \mathbf{B}(\mathbf{x}) \times \mathbf{S}. \quad (7)$$

This cross product describes a precession about the vector $\hat{\mathbf{B}}(\mathbf{x}) \approx \hat{\mathbf{k}}$ with a frequency of $\omega \approx g\mu_B B_0/\hbar$. So, the S_z component is left unchanged (in the first order), but the S_y contribution is under rapid oscillation. So, the B_0 term is the source of the decoupling. We would like to see this explicitly, and do so by defining a new phase altered wavefunction $\bar{\Psi}_{\pm}$ as

$$\Psi_{\pm}(\mathbf{x}, t) = e^{\mp ig\mu_B B_0 t/2\hbar} \bar{\Psi}_{\pm}(\mathbf{x}, t). \quad (8)$$

Then eq (??) becomes

$$-\frac{\hbar^2}{2m} \nabla^2 \bar{\Psi}_{\pm} \pm \frac{g\mu_B \beta y}{2i} e^{\pm ig\mu_B B_0 t/2\hbar} \bar{\Psi}_{\mp} \mp \frac{g\mu_B \beta z}{2} \bar{\Psi}_{\pm} = i\hbar \frac{\partial \bar{\Psi}_{\pm}}{\partial t}. \quad (9)$$

Compared to the time scale of the trajectory, the coupling term oscillates rapidly, and averages to zero. We are then left with

$$-\frac{\hbar^2}{2m} \nabla^2 \bar{\Psi}_{\pm} \mp \frac{g\mu_B \beta z}{2} \bar{\Psi}_{\pm} = i\hbar \frac{\partial \bar{\Psi}_{\pm}}{\partial t}. \quad (10)$$

If we now apply Ehrenfest's theorem to the two separate Hamiltonians ⁴, we get

$$\frac{d \langle \mathbf{x} \rangle_{\pm}}{dt} = \frac{\langle \mathbf{p} \rangle_{\pm}}{m} \text{ and } \frac{d \langle \mathbf{p} \rangle_{\pm}}{dt} = \pm \frac{g\mu_B \beta}{2} \hat{\mathbf{k}}. \quad (11)$$

In summary, this shows that not only are the spin components decoupled by the strong magnetic field, but we can measure macroscopically the distinct trajectories made by the two spin eigenstates.

APPENDIX B: CALCULATION OF THE GAP MAGNETIC FIELD

In the Stern Gerlach experiment, all of our final values are based on the calculation of the magnetic field gradient in the region between two cylindrical surfaces. A picture of the magnet orientation is shown in Fig. 5

⁴ $\frac{d \langle U \rangle}{dt} = (i\hbar)^{-1} \langle [\mathcal{H}, U] \rangle$

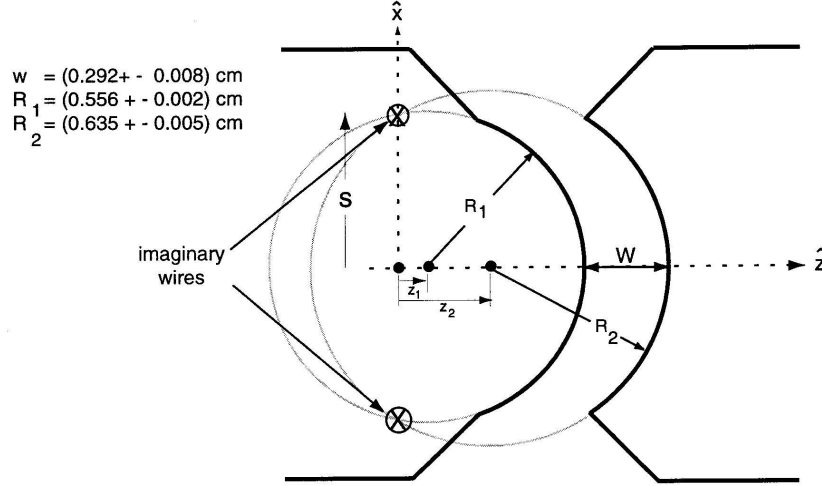


Figure 6: Top view of the experimental apparatus used in the Stern Gerlach experiment

In this experiment, we have a special setup of magnets where we can actually solve for the exact value of the magnetic field (See Figure 6). We will show that the solution is the same as from two wires carrying current parallel to the intersections of the two cylinders (we have labeled these points at $x = \pm s, z = 0$). We call the value of this imaginary current a , and we proceed to show that this causes the same magnetic field as our original setup. It turns out that this choice of wires automatically satisfies the condition that \mathbf{B} is always perpendicular to the cylindrical pieces, necessary because $\mu_0/\mu_{iron} \approx 0$ (and $\nabla \times \mathbf{B} = 0$ right?). From the theory of potential functions, if a potential satisfies all boundary conditions, it automatically describes the field everywhere inside the boundary, namely the magnet gap. From the geometry shown, we have three necessary geometric relations

$$s^2 + z_1^2 = R_1^2, \quad s^2 + z_2^2 = R_2^2, \quad z_1 + R_1 + W = z_2 + R_2. \quad (1)$$

At any point we need \mathbf{B} to be perpendicular to the cylindrical surface, a condition expressed by $B_x/B_z = -\partial z/\partial x$ (negative inverse slope). We now show that this condition is satisfied.

The outer surface is described by the equation

$$x^2 + (z - z_2)^2 = R_2^2, \quad (2)$$

so for this surface

$$-\left(\frac{\partial z}{\partial x}\right)_{outersurface} = \frac{x}{z - z_2}. \quad (3)$$

We compare this to B_x/B_z . Taking x and z -components of the field, we have four equations (in mks units)

$$B_{1,2\ x} = \frac{\mu_0 a}{2\pi} \frac{\pm z}{(x \mp s)^2 + z^2} \text{ and } B_{1,2\ z} = \frac{\mu_0 a}{2\pi} \frac{\mp(x \mp s)}{(x \mp s)^2 + z^2}. \quad (4)$$

We thus obtain

$$\frac{B_x}{B_z} = \frac{2zx}{z^2 - x^2 + s^2}. \quad (5)$$

Using the geometric facts mentioned in eq. (??), we find that this is equal to the expression in eq. (??). Noting that throughout the above calculation, we could have used R_1 instead of R_2 (because it cancels out of calculations), this shows that both the inner and outer boundary conditions are obeyed.

Now, we need to find the magnitude of the magnetic field, which we will solve only for the axis (we assume that in the experiment the deviation from the axis is less important than the deviation along the axis, which is a highly approximate solution, especially dealing with our standard error for particle distance from the center of the gap along the axis). The overall magnitude of B on the z -axis is

$$|B|_{onaxis} = \frac{\mu_0 a}{\pi} \frac{s}{s^2 + z^2}. \quad (6)$$

Then the gradient along the axis is

$$\frac{\partial B_z}{\partial z} = -\frac{2zB_z}{s^2 + z^2}. \quad (7)$$

The hysteresis curve that gives us the magnetic field from current was measured with a hall probe, at a point we call z_p . We want the field at the (assumed) point of the beam, z_c , so we must correct to that value. For our two points, we have the magnetic fields

$$B_{z_c} = \frac{\mu_0 a}{\pi} \frac{s}{s^2 + z_c^2}, \text{ and } B_{z_p} = \frac{\mu_0 a}{\pi} \frac{s}{s^2 + z_p^2}. \quad (8)$$

We can then substitute B_{z_p} by B_{z_c} so that we can use the calibrated hysteresis curve calculated before the experiment was performed. We find, from eq. ??,

$$B_{z_p} = \frac{s^2 + z_c^2}{s^2 + z_p^2} B_{z_c}. \quad (9)$$

Thus, our final expression for the magnetic field gradient used in the above lab analysis is given by

$$\left. \frac{\partial B_z}{\partial z} \right|_{z=z_c} = \frac{-2z_c(s^2 + z_p^2)B_{z_p}}{(s^2 + z_c^2)^2}. \quad (10)$$

We then, carrying through calculations, find as our expected error

$$\Delta \left(\frac{\partial B_z}{\partial z} \right) = \frac{\partial B_z}{\partial z} \sqrt{\left(\frac{\Delta z_c}{z_c} - \frac{4z_c \Delta z_c}{s^2 + z_c^2} \right)^2 + \left(\frac{2s \Delta s}{s^2 + z_p^2} - \frac{4s \Delta s}{s^2 + z_c^2} \right)^2 + \left(\frac{2z_p \Delta z_p}{s^2 + z_p^2} \right)^2 + \left(\frac{\Delta B_{z_p}}{B_{z_p}} \right)^2} \quad (11)$$

Solving the geometric relations, along with errors, yields us the values $z_1 = 0.11 \pm 0.01$ [cm], $z_2 = 0.33 \pm 0.02$ [cm], and $s = \sqrt{R_1^2 - z_1^2} = 0.54 \pm 0.03$ [cm]. This gives us measures for z_c and z_p , namely

$$z_c = z_2 + R_2 - w/2 = 0.82 \pm 0.05 \text{ cm} \quad (12)$$

and

$$z_p = z_2 + R_2 - w + .01'' = 0.70 \pm .03 \text{ cm}. \quad (13)$$

We summarize our final calculations in Table 2.

Some of these values are used in Table 1, where we calculate the magnetic moment of Potassium.

Current [A]	B_{z_p} [T]	Estimated error for B_{z_p}	$\frac{\partial B_z}{\partial z}$ [T/m]	Estimated error for $\frac{\partial B_z}{\partial z}$
1.1	2.1	9.5%	28.6	15.3%
2.12	4.5	4.4%	61.3	13.1%
3.2	6.8	2.9%	92.6	12.6%
4.23	8.0	2.5%	109.0	12.5%
5.32	8.9	2.2%	121.3	12.4%

TABLE II. Table 2: Calculations of Field Gradient for different applied currents.